

Article

Not peer-reviewed version

Processing of Bulk Hemp Seeds by Estimating the Optimum Input and Output Parameters and the Description of the Theoretical Deformation Energy Under Uniaxial Compression Loading

[Abraham Kabutey](#)^{*} , Mahmud Musayev , [Sonia Habtamu Kibret](#) , [Su Su Soe](#)

Posted Date: 7 January 2026

doi: 10.20944/preprints202601.0469.v1

Keywords: compression process; Box-Behnken design; response surface regression; mechanical properties; mathematical models



Preprints.org is a free multidisciplinary platform providing preprint service that is dedicated to making early versions of research outputs permanently available and citable. Preprints posted at Preprints.org appear in Web of Science, Crossref, Google Scholar, Scilit, Europe PMC.

Copyright: This open access article is published under a [Creative Commons CC BY 4.0 license](#), which permit the free download, distribution, and reuse, provided that the author and preprint are cited in any reuse.

Disclaimer/Publisher's Note: The statements, opinions, and data contained in all publications are solely those of the individual author(s) and contributor(s) and not of MDPI and/or the editor(s). MDPI and/or the editor(s) disclaim responsibility for any injury to people or property resulting from any ideas, methods, instructions, or products referred to in the content.

Article

Processing of Bulk Hemp Seeds by Estimating the Optimum Input and Output Parameters and the Description of the Theoretical Deformation Energy Under Uniaxial Compression Loading

Abraham Kabutey *, Mahmud Musayev, Sonia Habtamu Kibret and Su Su Soe

Department of Mechanical Engineering, Faculty of Engineering, Czech University of Life Sciences Prague, 165 20 Prague, Czech Republic

* Correspondence: kabutey@tf.czu.cz; Tel.: +420-22438-3180

Abstract

This present study adopted the Box-Behnken Design (BBD) with Response Surface Methodology (RSM) to identify the optimum input processing factors (heating temperature: 40, 50 and 60 °C, heating time: 30, 45 and 60 min and pressing height: 60, 80 and 100 mm) for estimating the oil output parameters (mass of oil, oil yield and oil expression efficiency) and deformation energy. The mechanical properties examined were the hardness and secant modulus of elasticity. Based on the full quadratic model, which includes both significant and non-significant terms, the optimal input processing factors were determined to be a heating temperature of 60 °C, a heating time of 52.5 min, and a sample pressing height of 100 mm, with coefficient of determination (R^2) values ranging from 0.68 to 0.95. The linear models with the significant terms predicted the mass of oil of 33.36 g, oil yield of 21.5 %, oil expression efficiency of 65.47 % and the experimental deformation energy of 1080.82 J. The percentage error values between the experimental and theoretical deformation energies were from 1.35 to 28.31%, suggesting that the varying input processing factors affected the coefficients of the tangent curve model for fitting the experimental force-deformation curves. The hardness and secant modulus of elasticity values ranged between 3.65 and 7.09 kN/mm and 123.98 to 150.39 MPa, indicating that the varying input processing factors had a significant effect on the stiffness of the bulk hemp seeds. These findings are useful for modelling and optimising the mechanical behaviour of oilseeds using a mechanical screw press to enhance oil recovery efficiency.

Keywords: compression process; Box-Behnken design; response surface regression; mechanical properties; mathematical models

1. Introduction

Hemp or industrial hemp (*Cannabis sativa* L.) is a multipurpose plant grown for many applications, including biofuel production [1–3]. It is a species in the Cannabaceae family in which the level of tetrahydrocannabinol (THC) is very low, according to the provisions under the Common Agricultural Policy (CAP) [4,5]. In the EU, the THC content is not allowed to exceed 0.3% of dry matter [4]. Hemp has been cultivated for millennia, dating back to approximately 10,000 years [6–9]. The hemp plant has grown across Europe for centuries mainly for textiles, ropes and other industrial applications, with a significant increase in cultivation from 20,540 ha in 2015 to 33,020 ha in 2022. In the same period, the production of hemp increased from 97,130 tonnes to 179,020 tonnes. France is the largest producer, accounting for more than 60% of EU production, followed by Germany (17%) and the Netherlands (5%) [4,5,10]. The global industrial hemp market size was estimated at USD 5.49 billion in 2023 and is projected to reach USD 16.82 billion by 2030, growing at a CAGR (Compound Annual Growth Rate) of 17.5% from 2024 to 2030 [11]. The growth is driven by the rising product

demand from application industries such as food and beverages, personal and animal care, across the globe. The top five hemp-producing countries in the world are China, Canada, the United States, France and Chile [12]. Hemp cultivation is beneficial for the environment and biodiversity due to its short cropping period, high resistance to harmful organisms, less water requirement compared to other fibre plants, and it can be grown in a wide range of weather and geographical conditions [13–15].

Hemp seeds, an edible hemp product, are notable for their oil (25–35%), protein (20–25%), carbohydrates (25–30%), insoluble fibre (10–15%) and an average phytate content of 2.80 g/100 g, which are of vital nutritional and bioactive importance [13,16]. Dehulled hemp seeds can contain up to 50% oil, with polyunsaturated fatty acids making up 80% of their total fatty acid content [13,17,18]. Hemp seeds are rich in polyunsaturated fatty acids, including omega-6 fatty acids, such as linoleic acid (18:2), and omega-3 fatty acids, particularly α -linolenic acid (18:3) [16]. In addition, hemp seeds are known to support overall health and exhibit anti-inflammatory properties. Omega-3 and omega-6 fatty acids offer protection against heart disease, alleviate inflammation in joints, aid in treating dermatitis, and contribute to maintaining skin moisture and balance [16,19].

The oil extraction process can be performed at room temperature (cold pressing) and increased temperature (hot pressing); the latter provides higher oil yield, but oil properties can be hindered at elevated temperatures [20]. Currently, both conventional and advanced technologies are used for oil extraction [21,22]. Conventional extraction methods such as screw press, Soxhlet extraction and hydro distillation have been used for extended periods. However, these methods are cost-effective in terms of machinery requirements, time-consuming extraction process, high energy requirement, greenhouse gas (GHG) emissions, considerable residual oil in oil press cakes and inferior oil quality [21,23,24]. Advanced methods, including enzyme-assisted, pulsed electric field pretreatment; microwave-assisted extraction, microwave-assisted hydro distillation, supercritical fluid extraction, ultrasound-assisted hydro distillation and sonication-assisted hydro distillation, are preferred to the conventional methods due to the lower requirement of the organic solvent, short extraction time, higher percentage oil recovery and retention of heat-sensitive compound quality of extract [21,25–31]. Particularly, to extract oil from hemp seeds, the screw press extraction, Soxhlet extraction, microwave-assisted solvent extraction and supercritical CO₂ have been utilised [16,32–36].

Another promising oil extraction technique is the uniaxial compression process [37], which has been utilized for extracting oil under cold and hot-pressing conditions from oil-bearing plant seeds/kernels such as flax, hemp, rape, pumpkin, hazelnut, sunflower and jatropha [38–43]. To understand the mechanical properties, oil recovery efficiency and deformation energy requirement of the oilseeds/nuts based on their experimental and theoretical force-deformation curves in relation to the varying input processing factors such as compressive force, speed, heating temperature, heating time, diameter of pressing vessel, samples pressing height and moisture content, it is ideal to use the uniaxial compression process. This process has not been adequately explored for hemp seeds coupled with optimization statistical techniques. The statistical optimization technique using response surface methodology combined with an experimental design such as Box-Behnken has been recently employed by several researchers to optimize the input processing factors and their corresponding output parameters [20,25,44–52]. Therefore, the objectives of the present study were to determine: the oil recovery efficiency, the mechanical properties, the theoretical deformation energy and the optimum input processing factors (heating temperature, heating time and pressing height) with their corresponding output parameters (mass of oil, oil yield, oil expression efficiency and experimental deformation energy) of bulk hemp seeds under uniaxial compression loading.

2. Materials and Methods

2.1. Sample

Samples of bulk hemp seeds were used for the study. The samples were purchased from Vitalcountry.cz, Plzeňská, Štěnovice, Czech Republic. The samples packaged in transparent plastic bags were kept under laboratory conditions before the experiments.

2.2. Determination of Moisture Content

The moisture content of the samples was determined using Eq. (1) [45,53].

$$MC = \left(\frac{m_b - m_a}{m_b} \right) \cdot 100 \quad (1)$$

where MC is the moisture content of samples (% w.b.), m_a and m_b are the masses of the samples before and after oven drying (g) for 17 h at 105 °C [54].

2.3. Determination of Oil Content

The oil content of the samples was determined using Eq. (2) following the Soxhlet extraction procedure with the use of petroleum ether [41,55–57].

$$OC = \left(\frac{m_o}{m_b} \right) \cdot 100 \quad (2)$$

where m_o is the mass of oil extracted (g) and m_b is the initial mass of the ground sample.

2.4. Box-Behnken Experimental Design

The input processing factors (heating temperature, heating time and pressing height) at three levels each were designed using STATISTICA 13 software [58] by employing the Box-Behnken experimental design (BBD) [59]. The heating temperature values were 40, 50 and 60 °C, the heating time values were 30, 45 and 60 min, and the pressing height values were 60, 80 and 100 mm. The overall design generated 17 experimental runs (Table 1) comprising twelve combinations of factors and five replications at the centre points using Eq. (3) [44,48,51].

Table 1. Box-Behnken experimental design with twelve combinations and five replications.

Run	Input processing factors			Coded values using Eq. (2)		
	H_{TP} (°C)	H_{TM} (min)	P_{HT} (mm)	H_{TP} (°C)	H_{TM} (min)	P_{HT} (mm)
1	40	30	80	-1	-1	0
2	60	30	80	1	-1	0
3	40	60	80	-1	1	0
4	60	60	80	1	1	0
5	40	45	60	-1	0	-1
6	60	45	60	1	0	-1
7	40	45	100	-1	0	1
8	60	45	100	1	0	1
9	50	30	60	0	-1	-1
10	50	60	60	0	1	-1
11	50	30	100	0	-1	1
12	50	60	100	0	1	1
13*	50	45	80	0	0	0
14*	50	45	80	0	0	0

15*	50	45	80	0	0	0
16*	50	45	80	0	0	0
17*	50	45	80	0	0	0

* Repetitions at the centre points of factor levels; H_{TP} : Heating temperature; H_{TM} : Heating time and P_{HT} : Initial pressing height of the sample.

$$N = 2k \times (k - 1) + C_0 \rightarrow 2 \times 3(3 - 1) + 5 = 17 \quad (3)$$

where k is the number of input factors and C_0 is the number of central points. The factors-levels stated above were coded from -1 (low value) to +1 (high value) with 0 being the centre value according to Eq. (4) [51,59,60].

$$x_i = \frac{X_i - X_0}{\Delta X} \quad (4)$$

where x_i is the coded value of the i^{th} variable, X_i is the uncoded value of the i^{th} test variable, X_0 is the uncoded value of the i^{th} test variable at the centre point, and ΔX is the step change in the real value of the variable i corresponding to the variation in a unit for the dimensionless value of the variable i . The polynomial regression model of a second order, defining the responses as a function of the input processing factors, is expressed in Eq. (5).

$$Y = \beta_0 + \sum_{i=1}^k \beta_i X_i + \sum_{i=1}^k \beta_{ii} X_i^2 + \sum_{i_1 < j}^k \sum_j^k \beta_{ij} X_i X_j \quad (5)$$

where Y is the response variable; $\beta_0, \beta_i, \beta_{ii}$ and β_{ij} are the regression coefficients of the intercept, linear, quadratic and interaction terms, respectively; X_i and X_j are the independent variables, and k is the number of factors.

2.5. Pretreatment of Samples Using Standard Oven

The samples of hemp seeds were preheated following the design presented in Table 1 using the standard oven equipment (MEMMERT GmbH + Co. KG, Buechenbach, Germany). The fan and the restrictor air flap in the oven were set at 30% to control the air circulation during the drying process.

2.6. Compression Tests of Samples After Pretreatment

The universal compression testing machine (ZDM 50, Czech Republic) of a maximum load of 500 kN and a pressing vessel of diameter 60 mm with a plunger were used for extracting the hemp seed oil (Figure 1a-c) following the Box-Behnken design (Table 1). Based on preliminary tests, the maximum input force required for hemp seeds was set at 300 kN at a pressing speed of 5 mm/min.

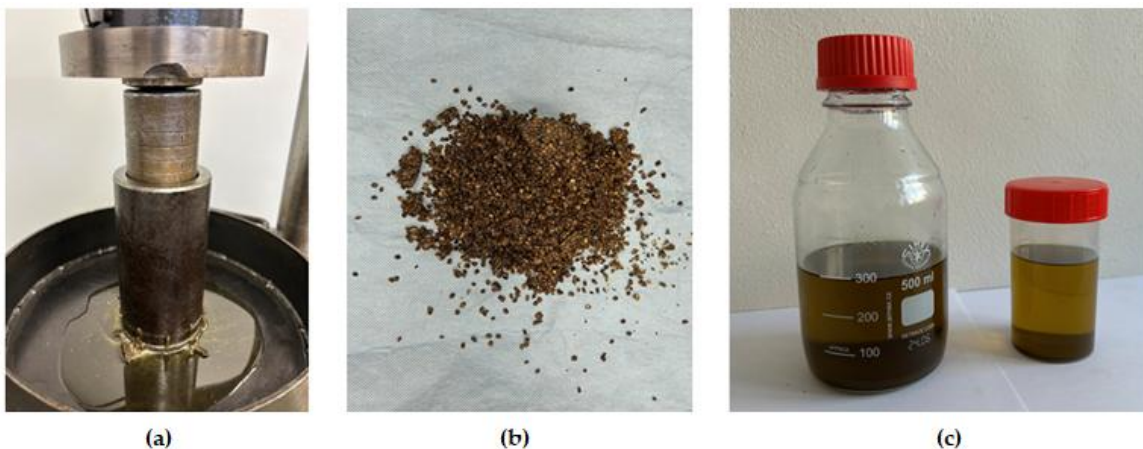


Figure 1. (a) Uniaxial compression test for extracting the oil, (b) seedcake of bulk hempseeds sample, (c) extracted oils from the 17 experimental tests/runs conducted.

2.6.1. Oil Yield

The oil yield was determined using Eq. (6) [25,59,61].

$$O_{YD} = \left[\left(\frac{M_{OL}}{M_{SP}} \right) \cdot 100 \right] \quad (6)$$

where O_{YD} is oil yield (%), M_{OL} is the mass of oil determined as the difference between the mass of the seedcake and the initial mass of the sample M_{SP} (g).

2.6.2. Oil Expression Efficiency

The oil expression efficiency was determined using Eq. (7) [62].

$$O_{EF} = \left[\left(\frac{O_{YD}}{O_{CT}} \right) \cdot 100 \right] \quad (7)$$

where O_{EF} is the oil expression efficiency (%) and O_{CT} is the percentage oil content (%) in the hemp seeds sample determined by Soxhlet extraction.

2.6.3. Deformation Energy

The deformation energy was determined using Eq. (8) [63–65].

$$E_{NG} = \sum_{n=0}^{n=i-1} \left[\left(\frac{F_{n+1} + F_n}{2} \right) \cdot (x_{n+1} - x_n) \right] \quad (8)$$

where E_{NG} is the deformation energy (J), $F_{n+1} + F_n$ and $x_{n+1} - x_n$ are the compressive force (kN) and deformation (mm), n is the number of data points, and i is the number of sections in which the axis deformation was divided.

2.6.4. Force and Deformation

The force, F_R (N) and deformation D_F (mm) values were obtained directly from the compression tests' output data.

2.6.5. Hardness

The hardness, H_{DN} (kN/mm) of the samples was calculated using Eq. (9) [53,66,67].

$$H_{DN} = \frac{F_{RC}}{D_{FX}} \quad (9)$$

2.6.6. Strain

The strain, ε_{ST} (-) of the samples was calculated using Eq. (10) [53,66,67].

$$\varepsilon_{ST} = \frac{D_{FX}}{H_{PT}} \quad (10)$$

2.6.7. Compressive Stress

The stress, σ_{SS} (MPa) of the samples was calculated using Eq. (11) [53,66,67].

$$\varepsilon_{ST} = \frac{F_{RC}}{A_{PV}} \quad (11)$$

where A_{PV} is the area of the pressing vessel, which was calculated to be 2827.43 mm².

2.6.8. Secant Modulus of Elasticity

The secant modulus of elasticity, E_{SM} of the samples was calculated based on Hooke's law using Eq. (12) [53,66,67].

$$E_{SM} = \frac{\sigma_{SS}}{\varepsilon_{ST}} \quad (12)$$

where E_{SM} is the secant modulus of elasticity (N/mm² = MPa) and ε_{ST} is the strain (-).

2.7. Utilisation of Tangent Curve Model

The tangent curve model (Eq. 13) [43] was used to describe the experimental force-deformation curves and energy of bulk hempseeds as a function of the input processing factors.

$$F_D(X) = A_D \cdot [\tan(B_D \cdot X)]^n \quad (13)$$

where $F_D(X)$ is the compression force (N) for the deformation of the bulk oilseeds, X (mm), A_D is the force coefficient of mechanical behaviour (N), B_D is the deformation coefficient of mechanical deformation behaviour (mm⁻¹) and n is the model's fitting exponent (-).

2.8. Statistical Analysis

The experimental data obtained were evaluated statistically using STATISTICA 13 [58] by employing the response surface regression technique at a 0.05 significance level. The theoretical fitting of the experimental force-deformation curves and the statistical metrics were done using MathCAD 14 (PTC Software, Needham, MA, USA) [43,68]. The graphical illustrations were also done by the above-mentioned statistical packages.

3. Results and Discussion

3.1. Calculated Moisture Content and Oil Content

The moisture content and the oil content of the samples of hemp seeds were determined to be 7.49 ± 0.08 (% w.b.) and 32.84 ± 0.70 %, respectively. The determined moisture content is within the optimum levels reported in the literature for different oilseeds before oil extraction. However, both higher and lower moisture content levels could result in an increase or a decrease in the percentage oil yield [69]. For instance, Moslavac et al. [69] mentioned that the lowest moisture content of 5.52 % produced the highest oil yield of rapeseeds in comparison with sunflower seeds, where the highest amount of oil yield was achieved at seeds moisture content of 6.77 %, which was also in agreement with the study reported by [Bambgoye and Adejumo (2011) [70] on sunflower seeds.

3.2. Calculated Responses from the BBD Experimental Runs

Following the BBD experimental runs in relation to the input processing factors combinations (Table 1), the calculated responses were the mass of oil, oil yield, oil expression efficiency and deformation energy using equations (Eq. 5) to (Eq. 7). The oil expression efficiency is dependent on the mass of oil, oil yield and oil content of the seeds, hence, the need to estimate all the oil output parameters. Based on the twelve factors combinations (runs 1 to 12) without any repetitions at the centre points, the highest amount of the oil expression efficiency of 67.27 % was obtained at run 6 (heating temperature: 60 °C, heating time: 45 min and pressing height of 60 mm) followed by run 10 (heating temperature: 50 °C, heating time: 60 min and pressing height of 60 mm) producing an amount of 65.12 % and then run 4 (heating temperature: 60 °C, heating time: 60 min and pressing height of 80 mm) generating 65.55%. However, the five repetitions of the input factors at the centre points recorded an average amount of 61.96 ± 4.08 %. Their corresponding deformation energies were 818.03, 722.55, 972.28 and 913.74 ± 55.04 J. It was observed that the highest deformation energies of 1179.6 and 1143.53 J were obtained from run 7 (heating temperature: 40 °C, heating time: 45 min and pressing height of 100 mm) and run 8 (heating temperature: 60 °C, heating time: 45 min and pressing

height of 100 mm) with oil expression efficiency amounts of 59.74 % and 65.12 % respectively. The area under the force-deformation curve (Figure 2) is the deformation energy for extracting the oil under uniaxial compression loading.

Table 2. Determined amounts of oil output parameters and deformation energy of bulk hempseeds from the BBD.

Run	Input processing factors			Calculated output parameters		
	H_{TP} (° C)	H_{TM} (min)	P_{HT} (mm)	M_{OL} (g)	O_{YD} (%)	O_{EE} (%)
1	40	30	80	20.53	15.94	48.55
2	60	30	80	26.46	20.55	62.57
3	40	60	80	25.26	19.62	59.73
4	60	60	80	27.72	21.53	65.55
5	40	45	60	20.87	21.15	64.40
6	60	45	60	21.8	22.09	67.27
7	40	45	100	31.88	19.62	59.74
8	60	45	100	34.75	21.39	65.12
9	50	30	60	20.96	21.24	64.68
10	50	60	60	21.37	21.66	65.94
11	50	30	100	32.26	19.85	60.45
12	50	60	100	31.25	19.23	58.56
13*	50	45	80	25.33	19.67	59.90
14*	50	45	80	25.15	19.53	59.47
15*	50	45	80	26.89	20.88	63.59
16*	50	45	80	24.73	19.20	58.48
17*	50	45	80	28.92	22.46	68.39
						886.46

* Repetitions at the centre points of factor levels; H_{TP} : Heating temperature; H_{TM} : Heating time; P_{HT} : Initial pressing height of sample; M_{OL} : Mass of oil extracted; O_{YD} : Percentage oil yield; O_{EE} : Percentage oil expression efficiency and E_{NG} : Deformation energy.

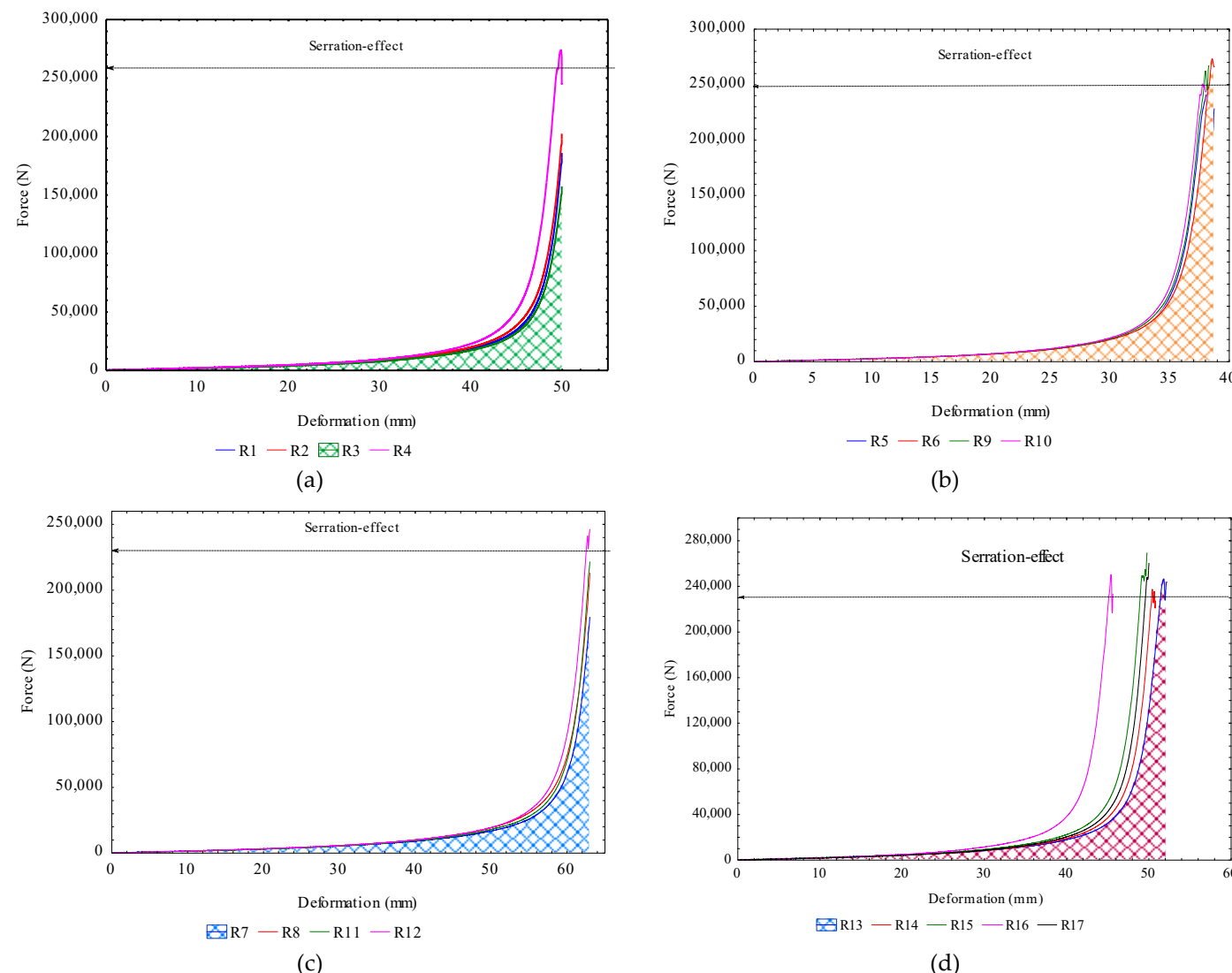


Figure 2. Force-deformation curves of bulk hempseeds at (a) various pressing heights (b) at various input processing factors at constant pressing height, $H = 80$ mm, (c) $H = 60$ mm, (d) $H = 100$ mm and (e) centre values of the input processing factors. The area under the curve represents the deformation energy.

3.3. Calculated Mechanical Properties from the Force-Deformation Curves

Each experimental run generated the force-deformation curve as shown in Figure 2a–d where the mechanical properties, namely the force, deformation, hardness, strain, stress and secant modulus of elasticity of the hemp seeds were calculated using equations (Eq. 8) to (Eq. 11) (Table 3). The hardness is dependent on the force and the deformation relation, whereas the secant modulus of elasticity is derived from the stress and strain ratio. The secant modulus is used for materials that exhibits non-linear relationship, and it thus explains the stiffness of the material, which is calculated over a specific operating range up to a chosen point on the non-linear curve [67]. Considering the mean values of the input factors center points (runs 13–17) and the individual input factors combinations (runs 1–12), the overall hardness and secant modulus of elasticity values ranged between 3.65 and 7.09 kN/mm and 123.98 to 150.39 MPa indicating that the varying input processing factors had significant effect on the stiffness of the bulk hemp seeds. It is important to mention that preceding the maximum compressive force is the serration-effect (Figure 2), which was characterised by the ejection of seedcake through the pressing holes mainly due to higher pressure leading to a vibration of the compression machine. Other factors such as moisture content, pressing speed, vessel diameter and quality of raw material could contribute to the serration effect characteristics [42,64,65]. Usually, the serration effect does not produce any significant amount of oil; hence, the compression process has to be discontinued to prevent insufficient use of input energy. The knowledge of the mechanical properties of oilseeds under the uniaxial compression process is relevant for understanding the pressure threshold in the screw press and its design and optimisation mechanisms [40,64–66,71].

Table 3. Determined mechanical properties of bulk hempseeds from the BBD.

Run	Input processing factors				Calculated output parameters				
	H_{TP} (° C)	H_{TM} (min)	P_{HT} (mm)	F_{RC} (kN)	D_{FX} (mm)	H_{DN} (kN/mm)	ϵ_{ST} (-)	σ_{ST} (MPa)	E_{SM} (MPa)
1	40	30	80	223.52	50.49	4.43	0.63	79.05	125.26
2	60	30	80	250.17	50.57	4.95	0.63	88.48	139.97
3	40	60	80	222.72	50.83	4.38	0.64	78.77	123.98
4	60	60	80	257.77	49.46	5.21	0.62	91.17	147.46
5	40	45	60	251.11	38.36	6.55	0.64	88.81	138.92
6	60	45	60	273.34	38.57	7.09	0.64	96.68	150.39
7	40	45	100	239.16	64.28	3.72	0.64	84.59	131.59
8	60	45	100	266.93	63.66	4.19	0.64	94.41	148.30
9	50	30	60	262.22	38.02	6.90	0.63	92.74	146.35
10	50	60	60	241.16	37.55	6.42	0.63	85.29	136.29
11	50	30	100	230.83	63.3	3.65	0.63	81.64	128.97
12	50	60	100	241.23	62.71	3.85	0.63	85.32	136.05
13*	50	45	80	246.62	51.81	4.76	0.65	87.22	134.68
14*	50	45	80	237.37	50.43	4.71	0.63	83.95	133.18
15*	50	45	80	249.49	49.17	5.07	0.61	88.24	143.57
16*	50	45	80	250.18	45.43	5.51	0.57	88.48	155.81
17*	50	45	80	248.00	49.87	4.97	0.62	87.71	140.70

* Repetitions at the centre points of factor levels; H_{TP} : Heating temperature; H_{TM} : Heating time; P_{HT} : Initial pressing height of sample; F_{RC} : Compression force; D_{FX} : Deformation; H_{DN} : Hardness; ϵ_{ST} : Strain; S_{TS} : Stress and E_{SM} : Secant modulus of elasticity.

3.4. ANOVA Analysis of Calculated Responses and Their Regression Coefficients

The ANOVA results of the response surface regression analysis of the calculated parameters (mass of oil, oil yield, oil expression efficiency and deformation energy) are provided in Tables 4 to 7. The coefficients of the intercept, linear, quadratic and interaction terms of the input processing factors (heating temperature, heating time and sample pressing height) for each parameter model showed both significant ($p\text{-value} < 0.05$) and non-significant ($p\text{-value} > 0.05$). For the mass of oil model parameter, the intercept, heating temperature and the sample pressing height indicated significant, whereas the other terms were non-significant. For the oil yield and oil expression efficiency model parameters, only the intercept and the heating temperature indicated significant, whereas the other terms were non-significant. The deformation energy model parameter showed that the intercept and the sample pressing height were significant, whereas the other terms were non-significant. The coefficient of determination (R^2) values confirm the models' coefficients ranged between 0.68 and 0.95, implying their adequacy for prediction.

Table 4. ANOVA results for the $M_{OL}(g)$ parameter at a 0.05 significance level.

Effect	Model ^a coefficients	Standard error	t-value	Sum of squares	df	Mean square	F- value	p- value
Intercept	26.20	0.77	33.89	292.5	9	32.50	10.87	0.00*
H_{TP} (L)	1.52	0.61	2.49	18.57	1	18.57	6.25	0.04*
H_{TP}^2 (Q)	-0.17	0.84	-0.21	0.13	1	0.13	0.04	0.84**
H_{TM} (L)	0.67	0.61	1.10	3.63	1	3.63	1.22	0.31**
H_{TM}^2 (Q)	-1.04	0.84	-1.23	4.54	1	4.54	1.53	0.26**
P_{HT} (L)	5.64	0.61	9.23	254.70	1	254.70	85.65	0.00*
P_{HT}^2 (Q)	1.29	0.84	1.54	7.05	1	7.05	2.37	0.17**
$H_{TP} \cdot H_{TM}$	-0.87	0.86	-1.00	3.01	1	3.01	1.01	0.35**
$H_{TP} \cdot P_{HT}$	0.49	0.86	0.56	0.94	1	0.94	0.32	0.59**
$H_{TM} \cdot P_{HT}$	-0.36	0.86	-0.41	0.50	1	0.50	0.17	0.69**
Residual				20.92	7	2.99		
Lack of Fit				9.03	3	3.01	1.01	0.47**
Pure Error				11.89	4	2.97		
Total				313.42	16			

H_{TP} : Heating temperature; H_{TM} : Heating time; P_{HT} : Initial pressing height of sample; L: Linear term;

Q: Quadratic term; ^a: Coefficient of determination (R^2) = 0.93 for mass of oil, $M_{OL}(g)$; *: $p\text{-value} < 0.05$

or higher F-value means significant and **: $p\text{-value} > 0.05$ or lower F-value means non-significant.

Table 5. ANOVA results for the $O_{YD}(\%)$ parameter at a 0.05 significance level.

Effect	Model ^a coefficients	Standard error	t-value	Sum of squares	df	Mean square	F- value	p- value
Intercept	20.35	0.59	34.40	25.6	9	2.84	1.62	0.00*
H_{TP} (L)	1.15	0.47	2.47	10.64	1	10.64	5.93	0.04*
H_{TP}^2 (Q)	-0.19	0.64	-0.29	0.15	1	0.15	0.08	0.78**
H_{TM} (L)	0.56	0.47	1.19	2.47	1	2.47	1.38	0.27**
H_{TM}^2 (Q)	-0.75	0.64	-1.17	2.39	1	2.39	1.33	0.28**
P_{HT} (L)	-0.76	0.47	-1.62	4.57	1	4.57	2.55	0.15**
P_{HT}^2 (Q)	0.90	0.64	1.40	3.41	1	3.41	1.90	0.21**
$H_{TP} \cdot H_{TM}$	-0.67	0.66	-1.02	1.82	1	1.82	1.01	0.34**
$H_{TP} \cdot P_{HT}$	0.21	0.66	0.31	0.17	1	0.17	0.09	0.76**
$H_{TM} \cdot P_{HT}$	-0.26	0.66	-0.39	0.27	1	0.27	0.15	0.71**

Residual		12.24	7	1.75			
Lack of Fit		5.07	3	1.69	0.94	0.49**	
Pure Error		7.17	4	1.79			
Total		37.82	16				

H_{TP} : Heating temperature; H_{TM} : Heating time; P_{HT} : Initial pressing height of sample; L: Linear term; Q: Quadratic term; ^a: Coefficient of determination (R^2) = 0.68 for oil yield, $O_{YD}(\%)$; *: p-value < 0.05 or higher F-value means significant and **: p-value > 0.05 or lower F-value means non-significant.

Table 6. ANOVA results for the $O_{EF}(\%)$ parameter at a 0.05 significance level.

Effect	Model ^a coefficients	Standard error	t-value	Sum of squares	df	Mean square	F- value	p- value
Intercept	61.96	1.80	34.40	237.2	9	26.35	1.62	0.00*
H_{TP} (L)	3.51	1.42	2.47	98.62	1	98.62	5.93	0.04*
H_{TP}^2 (Q)	-0.57	1.96	-0.29	1.37	1	1.37	0.08	0.78**
H_{TM} (L)	1.69	1.42	1.19	22.91	1	22.91	1.38	0.27**
H_{TM}^2 (Q)	-2.29	1.96	-1.17	22.17	1	22.17	1.33	0.28**
P_{HT} (L)	-2.30	1.42	-1.62	42.37	1	42.37	2.55	0.15**
P_{HT}^2 (Q)	2.74	1.96	1.40	31.59	1	31.59	1.90	0.21**
$H_{TP} \cdot H_{TM}$	-2.05	2.01	-1.02	16.83	1	16.83	1.01	0.34**
$H_{TP} \cdot P_{HT}$	0.63	2.01	0.31	1.57	1	1.57	0.09	0.76**
$H_{TM} \cdot P_{HT}$	-0.79	2.01	-0.39	2.49	1	2.49	0.15	0.71**
Residual				113.54	7	16.22		
Lack of Fit				47.02	3	15.67	0.94	0.49**
Pure Error				66.51	4	16.63		
Total				350.69	16			

H_{TP} : Heating temperature; H_{TM} : Heating time; P_{HT} : Initial pressing height of sample; L: Linear term; Q: Quadratic term; ^a: Coefficient of determination (R^2) = 0.68 for oil expression efficiency, $O_{EF}(\%)$; *: p-value < 0.05 or higher F-value means significant and **: p-value > 0.05 or lower F-value means non-significant.

Table 7. ANOVA results for $E_{NG}(J)$ parameter at a 0.05 significance level.

Effect	Model ^a coefficients	Standard error	t-value	Sum of squares	df	Mean square	F- value	p- value
Intercept	913.76	20.20	45.25	252777	9	28086.33	13.77	0.00*
H_{TP} (L)	24.94	15.97	1.56	4977	1	4977	1.64	0.16**
H_{TP}^2 (Q)	38.82	22.01	1.76	6345.4	1	6345.4	2.09	0.12**
H_{TM} (L)	-8.57	15.97	-0.54	587	1	587	0.19	0.61**
H_{TM}^2 (Q)	-38.22	22.01	-1.74	6151.2	1	6151.2	2.03	0.13**
P_{HT} (L)	167.06	15.97	10.46	223282.4	1	223282.4	73.58	0.00*
P_{HT}^2 (Q)	35.49	22.01	1.61	5304.2	1	5304.2	1.75	0.15**
$H_{TP} \cdot H_{TM}$	32.25	22.58	1.43	4159.6	1	4159.6	1.37	0.20**
$H_{TP} \cdot P_{HT}$	7.30	22.58	0.32	213	1	213	0.07	0.76**
$H_{TM} \cdot P_{HT}$	24.19	22.58	1.07	2340.6	1	2340.6	0.77	0.32**
Residual				14275.38	7	2039.34		
Lack of Fit				2137.3	3	712.4	0.23	0.87**

Pure	12138	4	3034.5
Error			
Total	267052.4	16	

H_{TP} : Heating temperature; H_{TM} : Heating time; P_{HT} : Initial pressing height of sample; L: Linear term;

Q: Quadratic term; a : Coefficient of determination (R^2) = 0.95 for deformation energy, $E_{NG}(J)$; * : p-

value < 0.05 or higher F-value means significant and ** : p-value > 0.05 or lower F-value means non-significant.

The coefficients of the full quadratic and reduced models are described in equations (Eq.14–Eq.21). The full quadratic models' coefficients, including both the significant and non-significant terms of the intercept, linear, quadratic and interactions (Eqs.14, 16, 18 and 20), are useful for identifying the optimal input factors. The adequacy of the full quadratic models was determined by the lack of fit P -values, which were greater than 0.05 (Tables 4 to 7). Similar evaluation of the quadratic model was reported in the studies by Todorovic et al. [20], [Chanioti and Tzia [59] and Ocholi et al.[60]. The reduced model coefficients comprising only the significant terms (Eqs.15, 17, 19 and 21) are effective for prediction and experimental validation. For mass of oil (Eq. 15), the dominant effect was the heating temperature and pressing height, whereas for oil yield (Eq. 17), and oil expression efficiency (Eq. 19), the dominant effect was the heating temperature, and for deformation energy (Eq. 21), the dominant effect was the pressing height.

$$M_{OL}(g) = 26.20 + 1.52 \cdot H_{TP} - 0.17 \cdot H_{TP}^2 + 0.67 \cdot H_{TM} - 1.04 \cdot H_{TM}^2 + 5.64 \cdot P_{HT} + 1.29 \cdot P_{HT}^2 - 0.87 \cdot H_{TP} \cdot H_{TM} + 0.49 \cdot H_{TP} \cdot P_{HT} - 0.36 \cdot H_{TM} \cdot P_{HT} \quad (14)$$

$$M_{OL}(g) = 26.20 + 1.52 \cdot H_{TP} + 5.64 \cdot P_{HT} \quad (15)$$

$$O_{YD}(\%) = 20.35 + 1.15 \cdot H_{TP} - 0.19 \cdot H_{TP}^2 + 0.56 \cdot H_{TM} - 0.75 \cdot H_{TM}^2 - 0.76 \cdot P_{HT} + 0.90 \cdot P_{HT}^2 - 0.67 \cdot H_{TP} \cdot H_{TM} + 0.21 \cdot H_{TP} \cdot P_{HT} - 0.26 \cdot H_{TM} \cdot P_{HT} \quad (16)$$

$$O_{YD}(\%) = 20.35 + 1.15 \cdot H_{TP} \quad (17)$$

$$O_{EF}(\%) = 61.96 + 3.51 \cdot H_{TP} - 0.57 \cdot H_{TP}^2 + 1.69 \cdot H_{TM} - 2.29 \cdot H_{TM}^2 - 2.30 \cdot P_{HT} + 2.74 \cdot P_{HT}^2 - 2.05 \cdot H_{TP} \cdot H_{TM} + 0.63 \cdot H_{TP} \cdot P_{HT} - 0.79 \cdot H_{TM} \cdot P_{HT} \quad (18)$$

$$O_{EF}(\%) = 61.96 + 3.51 \cdot H_{TP} \quad (19)$$

$$E_{NG}(J) = 913.76 + 24.94 \cdot H_{TP} + 38.82 \cdot H_{TP}^2 - 8.57 \cdot H_{TM} - 38.22 \cdot H_{TM}^2 + 167.06 \cdot P_{HT} + 35.49 \cdot P_{HT}^2 + 32.25 \cdot H_{TP} \cdot H_{TM} + 7.30 \cdot H_{TP} \cdot P_{HT} + 24.19 \cdot H_{TM} \cdot P_{HT} \quad (20)$$

$$E_{NG}(J) = 913.76 + 167.06 \cdot P_{HT} \quad (21)$$

3.5. Profiles of Predicted Values Based on Optimal Input Factors and Desirability

The predicted and desirability profiles of the full quadratic models are illustrated in Figures 3–6, respectively. The mass of oil regression model (Eq. 14) predicted an amount of 34.976 g with the optimal input factors (heating temperature: 60 °C (+1), heating time: 45 min (0) and sample pressing height: 100 mm (+1)) with a desirability value of 1 (Figure 3). The oil yield regression model (Eq. 16) predicted an amount of 22.647 % with optimal input factors (heating temperature: 60 °C (+1), heating time: 52.5 min (0.5) and sample pressing height: 60 mm (-1)), achieving the desirability value of 1 (Figure 4). The oil expression efficiency regression model (Eq. 18) predicted an amount of 68.96 % with optimal input factors (heating temperature: 60 °C (+1), heating time: 52.5 min (0.5) and sample

pressing height: 60 mm (-1) achieving the desirability value of 1 (Figure 5). The deformation energy regression model (Eq. 20) predicted an amount of 1197 (J) with optimal input factors (heating temperature: 60 °C (+1), heating time: 60 min (+1) and sample pressing height: 100 mm (+1)), giving the desirability value of 1 (Figure 6). The desirability value of 1 was identified in all cases, implying that all the responses simultaneously achieved their individual optima without any existence of trade-offs [59,60]. However, the reduced regression models (Eqs.15, 17, 19 and 21), considering only the significant terms from the full quadratic models, produced the mass of oil of 33.36 g, oil yield of 21.5 %, oil expression efficiency of 65.47 % and deformation energy of 1080.82 J. The differences between the full quadratic model and the reduced model predictions were determined using absolute and relative differences (Table 8). For all the model responses, relative differences were below 10%, indicating close agreement between the two regression models.

Table 8. Prediction comparison between the full quadratic model and the reduced model.

Model responses	Full quadratic model (Eqs.14, 16, 18 and 20)	Reduced model (Eqs.15, 17, 19 and 21)	Absolute difference	Relative difference (%)
$M_{OL}(g)$	34.98	33.36	1.62	4.62
$O_{YD}(\%)$	22.65	21.50	1.15	5.06
$O_{EE}(\%)$	68.96	65.47	3.49	5.06
$E_{NG}(J)$	1197.00	1080.82	116.18	9.71

M_{OL} : Mass of oil; O_{YD} : Oil yield; O_{EE} : Oil expression efficiency and E_{NG} : Deformation energy.

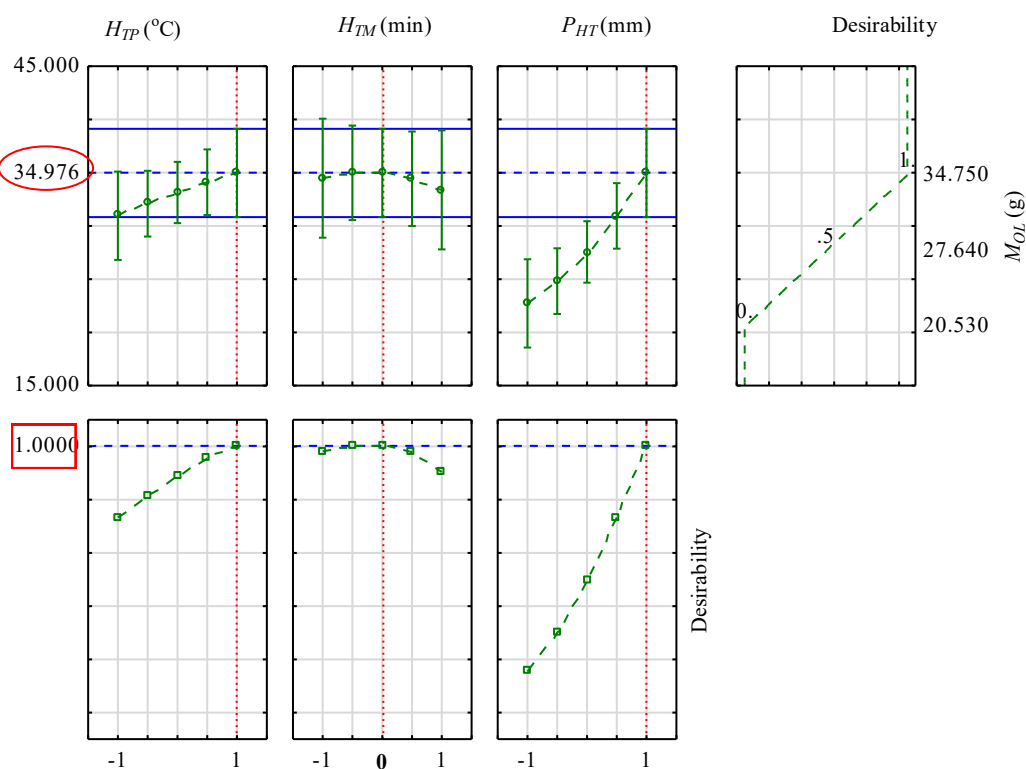


Figure 3. Profiles of predicted values (blue dotted lines) and desirability (red dotted lines) of the mass of oil, M_{OL} parameter; H_{TP} : Heating temperature (+1: optimal level of 60 °C); H_{TM} : Heating time (0: optimal level of 45 min) and P_{HT} : Initial pressing height of sample (+1: optimal level of 100 mm). The dotted blue line.

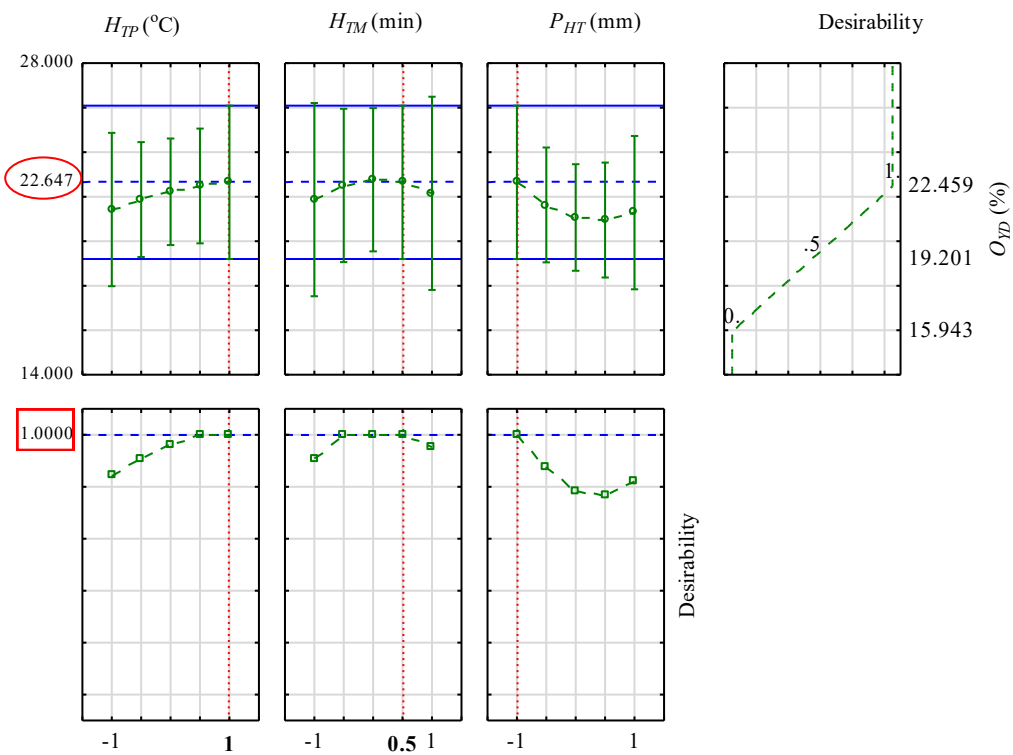


Figure 4. Profiles of predicted values (blue dotted lines) and desirability (red dotted lines) of oil yield, O_{YD} parameter; H_{TP} : Heating temperature (+1: optimal level of 60 $^{\circ}\text{C}$); H_{TM} : Heating time (0.5: optimal level of 52.5 min) and P_{HT} : Initial pressing height of sample (-1: optimal level of 60 mm).

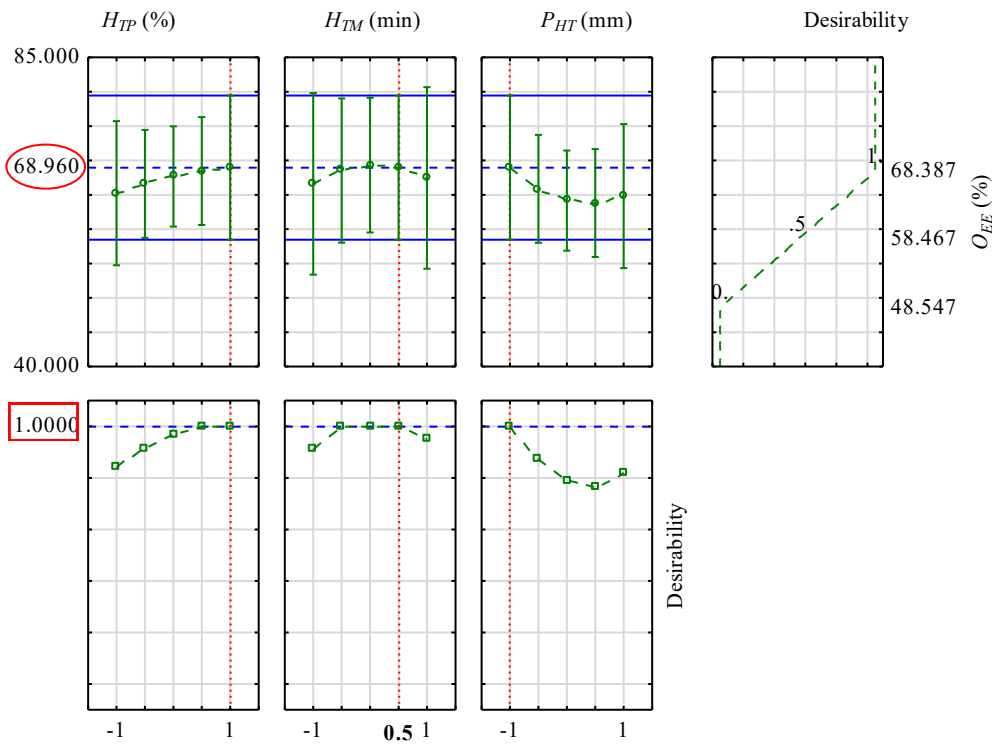


Figure 5. Profiles of predicted values (blue dotted lines) and desirability (red dotted lines) of oil expression efficiency, O_{EE} parameter; H_{TP} : Heating temperature (+1: optimal level of 60 $^{\circ}\text{C}$); H_{TM} : Heating time (0.5: optimal level of 52.5 min) and P_{HT} : Initial pressing height of sample (-1: optimal level of 60 mm).

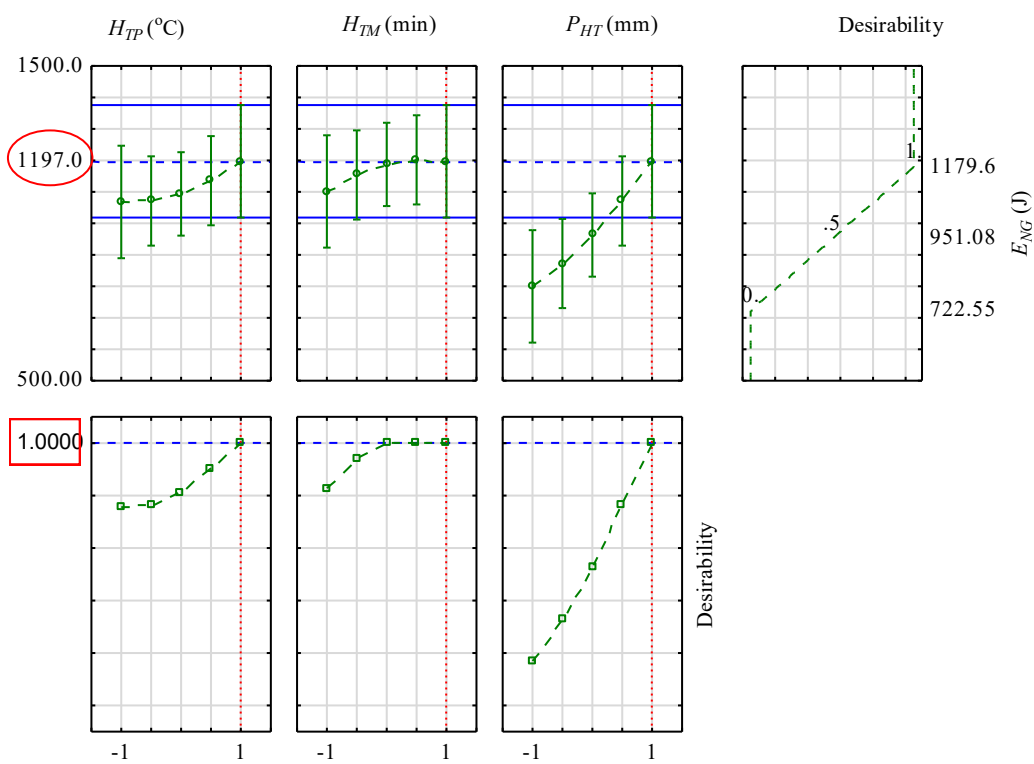


Figure 6. Profiles of predicted values (blue dotted lines) and desirability (red dotted lines) of deformation energy, E_{NG} parameter; H_{TP} : Heating temperature (+1: optimal level of 60 °C); H_{TM} : Heating time (+1: optimal level of 60 min) and P_{HT} : Initial pressing height of sample (+1: optimal level of 100 mm).

3.6. Observed, Predicted, Residuals and Percentage Error

The residuals from the observed and predicted based on the full quadratic models (Eqs.11, 13, 15 and 17) for the individual experimental runs and their percentage error are presented in Tables 9 and 10 and subsequently illustrated in Figure 7a-h. A positive residual means the model underpredicts the observed value, whereas a negative residual means the model overpredicts the observed value. However, randomly distributed residuals around the zero line and the lower percentage error values between 0.14 and 10.52 indicate a good model performance [45].

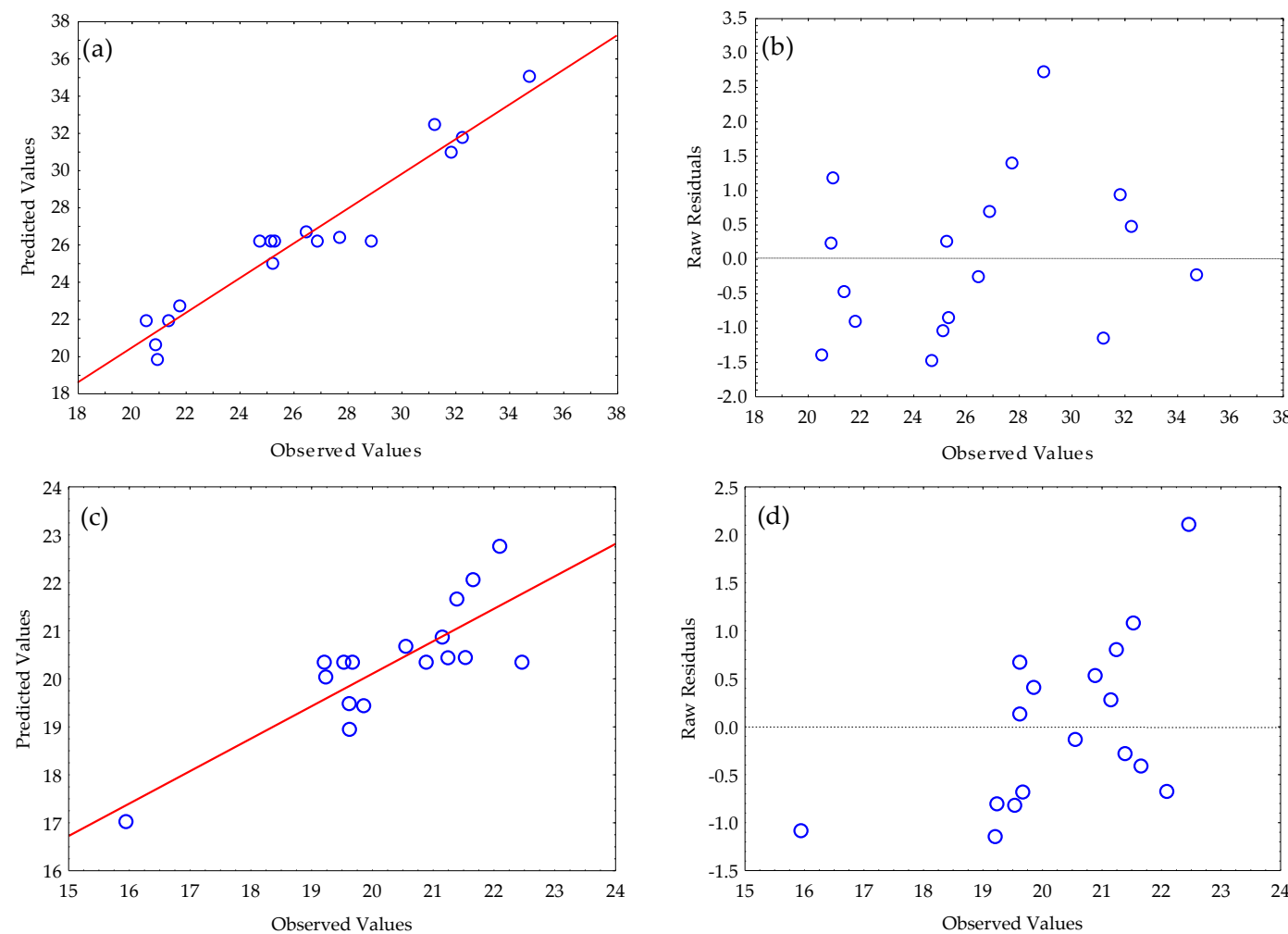
Table 9. Observed, predicted, residuals and absolute percentage error values of mass of oil and oil yield.

Runs	Mass of oil, $M_{OL}(g)$				Oil yield, $O_{YD}(\%)$			
	Observed	Predicted	Residuals	% Error	Observed	Predicted	Residuals	% Error
1	20.53	21.93	-1.40	6.37	15.94	17.03	-1.08	6.36
2	26.46	26.71	-0.25	0.94	20.55	20.68	-0.13	0.64
3	25.26	25.01	0.25	1.00	19.62	19.48	0.13	0.67
4	27.72	26.32	1.40	5.31	21.53	20.44	1.08	5.30
5	20.87	20.64	0.23	1.10	21.15	20.87	0.28	1.34
6	21.80	22.72	-0.92	4.05	22.09	22.76	-0.67	2.96
7	31.88	30.96	0.92	2.98	19.62	18.95	0.67	3.55
8	34.75	34.98	-0.23	0.65	21.39	21.66	-0.28	1.29
9	20.96	19.79	1.17	5.92	21.24	20.44	0.80	3.94

10	21.37	21.85	-0.48	2.18	21.66	22.07	-0.41	1.86
11	32.26	31.78	0.48	1.50	19.85	19.44	0.41	2.11
12	31.25	32.42	-1.17	3.61	19.23	20.04	-0.80	4.01
13	25.33	26.20	-0.87	3.34	19.67	20.35	-0.68	3.34
14	25.15	26.20	-1.05	4.02	19.53	20.35	-0.82	4.02
15	26.89	26.20	0.69	2.62	20.88	20.35	0.53	2.62
16	24.73	26.20	-1.47	5.63	19.20	20.35	-1.14	5.63
17	28.92	26.20	2.72	10.36	22.46	20.35	2.11	10.36

Table 10. Observed, predicted, residuals and absolute percentage error values of oil expression efficiency and deformation energy.

Runs	Oil expression efficiency, O_{EE} (%)				Deformation energy, E_{NG} (J)			
	Observed	Predicted	Residuals	% Error	Observed	Predicted	Residuals	% Error
1	48.55	51.85	-3.30	6.36	920.94	930.23	-9.29	1.00
2	62.57	62.97	-0.40	0.64	934.74	915.62	19.12	2.09
3	59.73	59.33	0.40	0.67	829.49	848.61	-19.12	2.25
4	65.55	62.25	3.30	5.30	972.28	962.99	9.29	0.97
5	64.40	63.55	0.85	1.34	811.15	803.37	7.78	0.97
6	67.27	69.32	-2.05	2.96	818.03	838.66	-20.63	2.46
7	59.74	57.69	2.05	3.55	1143.53	1122.90	20.63	1.84
8	65.12	65.97	-0.85	1.29	1179.60	1187.38	-7.78	0.66
9	64.68	62.23	2.45	3.94	778.24	776.73	1.51	0.19
10	65.94	67.19	-1.25	1.86	722.55	711.22	11.33	1.59
11	60.45	59.21	1.25	2.11	1051.14	1062.48	-11.34	1.07
12	58.56	61.01	-2.45	4.01	1092.21	1093.72	-1.51	0.14
13	59.90	61.96	-2.07	3.34	1009.92	913.76	96.16	10.52
14	59.47	61.96	-2.49	4.02	876.28	913.76	-37.48	4.10
15	63.59	61.96	1.62	2.62	909.25	913.76	-4.51	0.49
16	58.48	61.96	-3.49	5.63	886.91	913.76	-26.85	2.94
17	68.39	61.96	6.42	10.36	886.46	913.76	-27.30	2.99



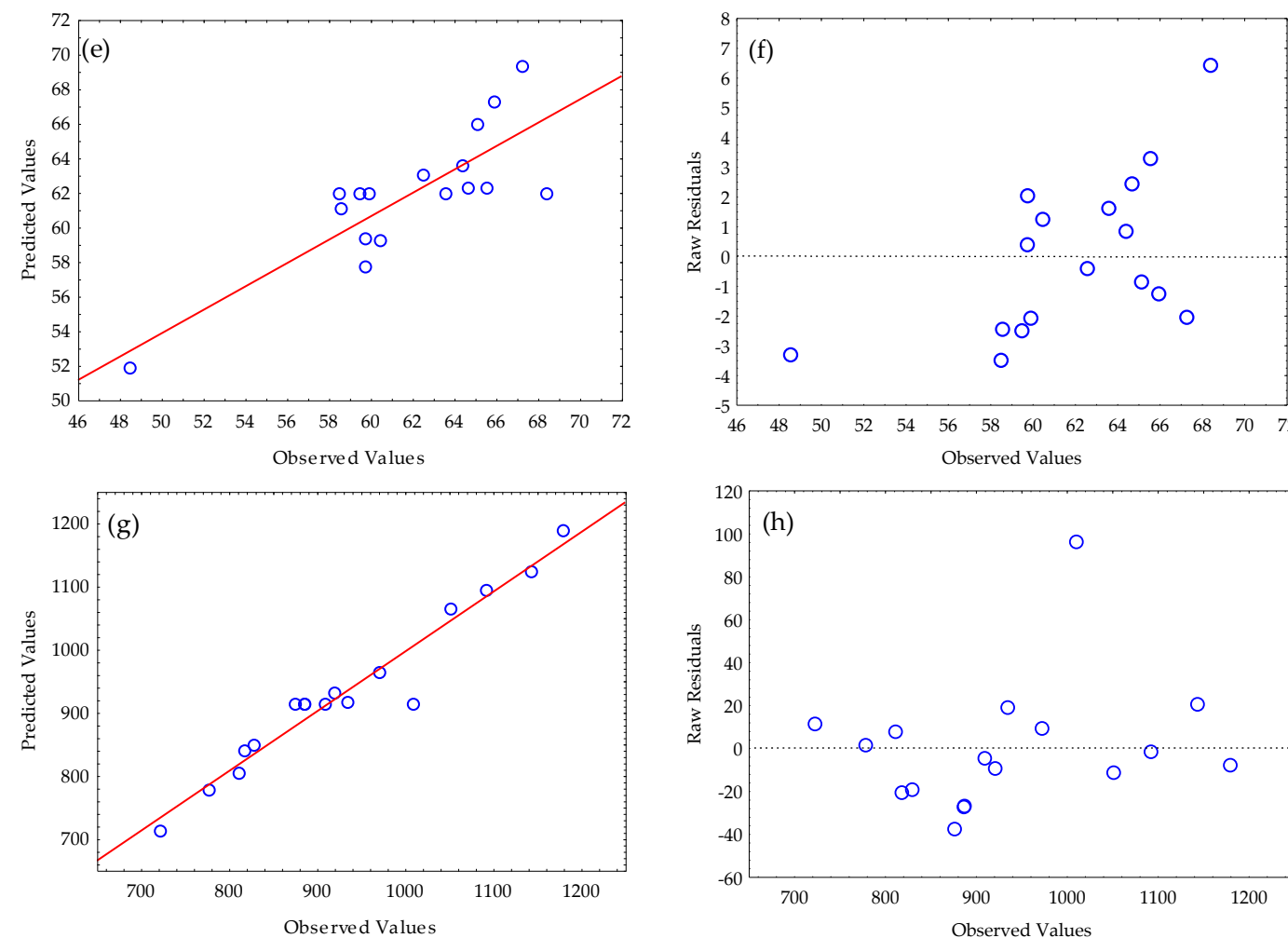


Figure 7. Observed versus predicted and observed versus residuals of mass of oil (a, b), oil yield (c, d), oil expression efficiency (e, f) and deformation energy (g, h).

3.7. Theoretical Force-Deformation Curves and Deformation Energy

The experimental force-deformation curves were described theoretically by employing the tangent curve model (Eq.13). The determined coefficients and statistical metrics of the model are presented in Table 7. The force coefficients of mechanical behaviour, A_D (kN) ranged from 2.504 and 4.26 kN whiles the deformation coefficients of mechanical behaviour, B_D ranged from 0.023 to 0.039 (mm^{-1}). The fitting exponent value of the tangent model was found to be 2, which defines the shape or steepness of the force-deformation curve. The force coefficient of the mechanical behaviour influences the slope of the deformation characteristic, whereas the deformation coefficient of mechanical behaviour influences the range of deformation. These two coefficients indicate the initial rigidity of the pressing process [43]. The tangent model coefficients were statistically significant (F-value < F-critical or P-value > 0.05) with high coefficients of determination (R^2), confirming their adequacy for describing the mechanical behaviour of bulk oilseeds or bulk agricultural materials under compression loading. The experimental and theoretical fitted curves for runs 1–4 are shown in Figure 7, which were similar to experimental runs 5–17.

Table 7. Determined coefficients of the tangent curve model and statistical metrics for describing the force-deformation curve of bulk hempseeds against the input processing factors of the BBD.

Run	X (mm)	A_D (kN)	B_D (mm^{-1})	n (-)	F-value	F-critical	P-value	R^2
1	50.49	2.759	0.029	2	1.341	3.851	0.247	0.993
2	50.57	3.094	0.029	2	0.882	3.851	0.348	0.995
3	50.83	2.687	0.029	2	0.946	3.851	0.331	0.995
4	49.46	3.477	0.029	2	0.695	3.851	0.405	0.996
5	38.36	4.260	0.038	2	0.184	3.851	0.668	0.989
6	38.57	4.000	0.038	2	0.327	3.851	0.368	0.996
7	64.28	2.895	0.023	2	0.630	3.851	0.428	0.991
8	63.66	2.923	0.023	2	0.913	3.851	0.340	0.995
9	38.02	3.809	0.038	2	0.458	3.851	0.499	0.995
10	37.55	3.726	0.039	2	0.633	3.851	0.427	0.996
11	63.30	2.504	0.023	2	1.202	3.851	0.273	0.993
12	62.71	2.867	0.023	2	1.101	3.851	0.294	0.995
13	51.81	3.487	0.028	2	0.532	3.851	0.466	0.993
14	50.43	2.913	0.029	2	0.963	3.851	0.327	0.995
15	49.17	3.166	0.030	2	0.872	3.851	0.351	0.996
16	45.43	3.724	0.032	2	0.407	3.851	0.524	0.996
17	49.87	2.899	0.029	2	0.835	3.851	0.361	0.995

X is the experimental deformation, D_{FX} (mm), A_D is the force coefficient of mechanical behaviour (kN), B_D is the deformation coefficient of mechanical behaviour (mm^{-1}), n is the model's fitting exponent (-), F-value < F-critical or P-value > 0.05 means significant, and R^2 is the coefficient of determination of the tangent model.

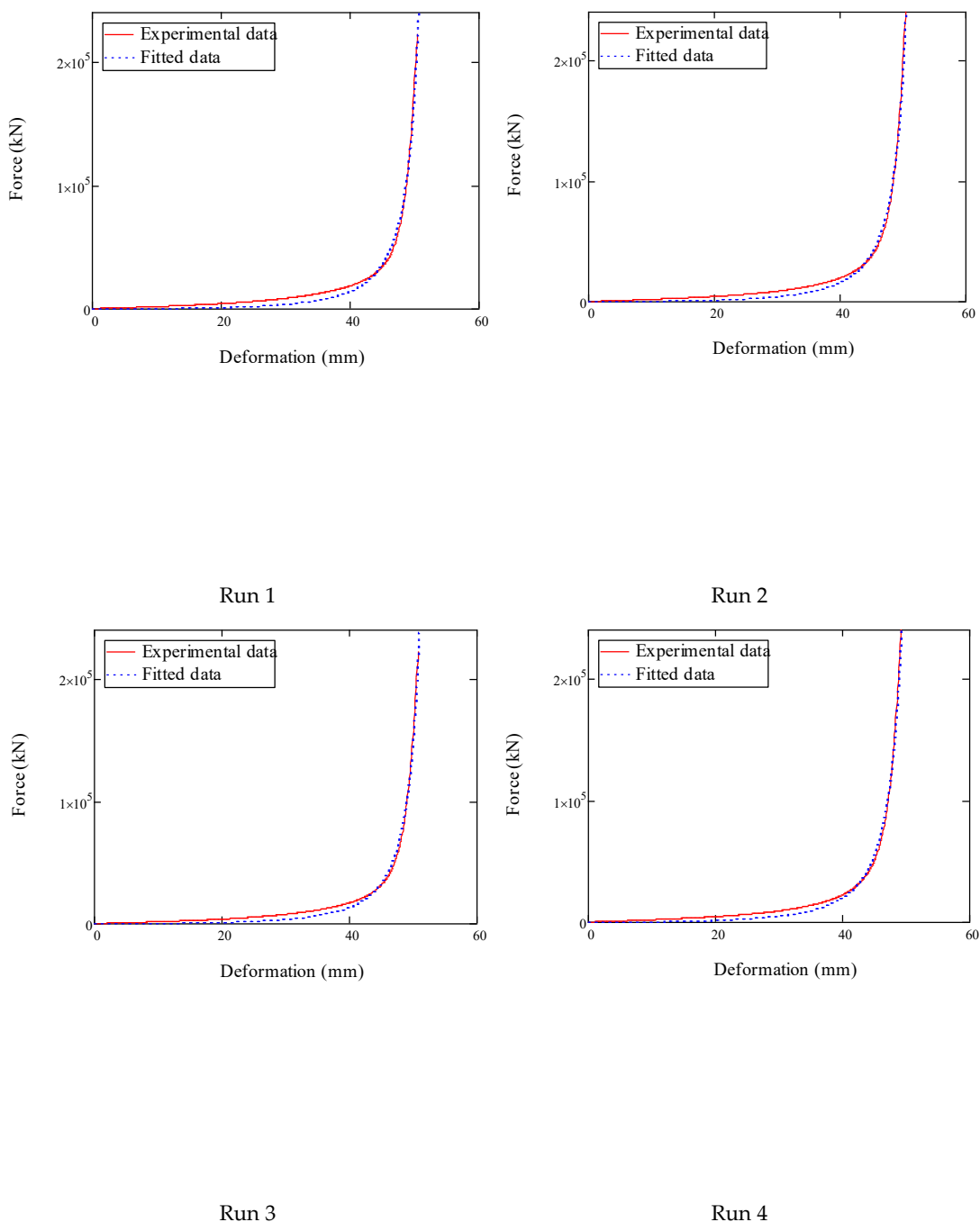


Figure 7. Experimental and fitted data of the force-deformation curves of bulk hempseeds for runs 1–4 representing similar curves obtained for experimental runs 5–17.

Based on the theoretically fitted curves, the theoretical deformation energies were calculated (Table 8) using the integral form of Eq. (13) as expressed in Eq. (22) for $n = 2$.

$$\int F(X)dx \rightarrow \frac{A \cdot (\tan(B \cdot X) - B \cdot X)}{B} \quad (22)$$

The percentage error values between the experimental and theoretical deformation energies ranged from 1.35 and 28.31%, suggesting that the varying input processing factors thus influence the coefficients of the tangent model. However, the efficiency of the tangent model was between 98.65% and 71.69%, which confirms its suitability for describing the mechanical behavior of oilseeds [43,72,73].

Table 8. Determined amounts of experimental and theoretical energy of bulk hempseeds against the input processing factors of the BBD.

Run	Input processing factors			Experimental and theoretical energy		
	H_{TP} (° C)	H_{TM} (min)	P_{HT} (mm)	E_{NG} (J)	TE_{NG} (J)	Error (%)
1	40	30	80	850.18	749.91	11.79
2	60	30	80	934.71	863.07	7.66
3	40	60	80	829.50	818.34	1.35
4	60	60	80	972.37	701.21	27.89
5	40	45	60	811.21	823.42	1.50
6	60	45	60	818.06	843.24	3.08
7	40	45	100	1141.28	1170	2.52
8	60	45	100	1179.66	1001	15.14
9	50	30	60	778.22	646.27	16.69
10	50	60	60	722.49	749.91	4.51
11	50	30	100	1051.16	784.87	25.33
12	50	60	100	1095.25	785.18	28.31
13	50	45	80	1009.84	851.14	15.72
14	50	45	80	876.21	776.742	11.35
15	50	45	80	909.29	943.75	3.79
16	50	45	80	886.90	820.62	7.47
17	50	45	80	886.16	653.78	26.22

H_{TP} : Heating temperature; H_{TM} : Heating time; P_{HT} : Initial pressing height of sample; E_{NG} :

Experimental deformation energy, TE_{NG} : Theoretical deformation energy.

4. Conclusions

The processing of bulk hemp seeds under uniaxial compression loading by applying the Box-Behnken Design and response surface methodology revealed the following findings. The maximum compressive force of 273.34 kN was obtained at the input factor combinations (heating temperature: 60 °C, heating time: 45 min and pressing height: 60 mm) in the absence of the serration-effect behaviour characterised by seedcake ejection without oil yield. Full quadratic and reduced (linear) regression models were described for the mass of oil, oil yield, oil expression efficiency and deformation energy. The quadratic models of a second order included both the significant and non-significant terms of the intercept, linear, quadratic and interactions of the input factors for assessing the models adequacy based on the lack-of-fit p-values > 0.05 . The linear models included only the significant terms useful for prediction and experimental validation. Based on the full quadratic models, the mass of oil was predicted as 34.976 g at optimal factor levels (heating temperature: 60 °C (+1), heating time: 45 min (0) and sample pressing height: 100 mm (+1)). The oil yield was predicted as 22.647 g at optimal factor levels (heating temperature: 60 °C (+1), heating time: 52.5 min (0.5) and sample pressing height: 60 mm (-1)). The oil expression efficiency was predicted at 68.96 (%) with optimal factor levels (heating temperature: 60 °C (+1), heating time: 52.5 min (0.5) and sample pressing height: 60 mm (-1)). The energy was predicted as 1197 (J)) at optimal factor levels (heating temperature: 60 °C (+1), heating time: 60 min (+1) and sample pressing height: 100 mm (+1)). All the optimal factor levels achieved a desirability value of 1, and the coefficient of determination (R^2) values were between 0.68 and 0.95, indicating the models' adequacy. The tangent curve model showed a good fit for describing the experimental force-deformation curves with (R^2) values closer to 1. However, the theoretical deformation energies obtained from the tangent curve model compared to the experimental deformation energies showed percentage error values between 1.35 and 28.31%,

which indicated that the varying input factors tend to affect the coefficients of the tangent curve model. The study approach will be validated in the mechanical screw press by modelling and optimizing the input processing factors in relation to the oil recovery efficiency and minimum energy requirement. The results of the present study are an expansion of the conference paper [74] in the proceeding of 9th International Conference on Trends in Agricultural Engineering 2025.

Author Contributions: A.K: Conceptualisation, Methodology, Supervision, Project administration, Funding acquisition, Formal analysis, Visualisation, Validation, Writing-Original Draft, Writing-Review & Editing. M.M: Investigation, Data curation, Formal analysis, Writing-Original Draft, Writing-Review & Editing. S.H.K.: Investigation, Data curation, Formal analysis, Writing-Original Draft, Writing-Review & Editing. S.S.S.: Investigation, Data curation, Formal analysis, Writing-Original Draft, Writing-Review & Editing. All authors have read and agreed to the published version of the manuscript.

Funding: The study was supported financially by the Internal Grant Agency of the Czech University of Life Sciences Prague (IGA Project Number – 2024:31130/1312/3108).

Institutional Review Board Statement: Not applicable.

Informed Consent Statement: Not applicable.

Data Availability Statement: The original contributions presented in the study are included in the article, further inquiries can be directed to the corresponding author.

Conflicts of Interest: The authors declare no conflicts of interest.

References

1. Dudziec, P.; Warminski, K.; Stolarski, M.J. Industrial hemp as a multipurpose crop: Last achievements and research in 2018 –2023. *Journal of Natural Fibres*. **2024**, *21*(1), 1–46.
2. Kolodziej, J.; Pudelko, K.; Mankowski, J. Energy and biomass yield of industrial hemp (*Cannabis sativa* L.) as influenced by seeding rate and harvest time in Polish agro-climatic conditions. *Journal of Natural Fibres*. **2023**, *20*(1), 1–11.
3. Andre, C.M.; Hausman, J-F.; Guerriero, G. *Cannabis sativa*: The plant of the thousand and one molecules. *Front. Plant Sci.* **2016**, *7*(19), 1–17.
4. Hemp - Agriculture and rural development - European Commission, accessed on 05/12/2025.
5. Pisanti, S.; Malfitano, A.M.; Ciaglia, E.; Lamberti, A.; Ranieri, R.; Cuomo, G.; Abate, M.; Faggina, G.; Proto, M.C.; Fiore, D.; Laezza, C.; Bifulco, M. Cannabidiol: State of the art and new challenges for therapeutic applications. *Pharmacology and Therapeutics*. **2017**, *175*, 133–150.
6. Michels, M.; Brinkmann, MuBhoff, O. Economic, ecological and social perspectives of industrial hemp cultivation in Germany: A qualitative analysis. *Journal of Environmental Management*. **2025**, *389*, 126117.
7. Berardo, M.E.V.; Mendieta, J.R.; Villamonte, M.D.; Colman, S.L.; Nercessian, D. Antifungal and antibacterial activities of *Cannabis sativa* L. resins. *Journal of Ethnopharmacology*. **2024**, *318*, 116839.
8. Pieracci, Y.; Ascrizzi, R.; Terreni, V.; Pistelli, L.; Flamini, G.; Bassolino, L.; Fulvio, F.; Montanari, M.; Paris, R. Essential oil of *Cannabis sativa* L.: Composition of yield and chemical composition of 11 hemp genotypes. *Molecules*. **2021**, *26*, 4080.
9. Schultes, R.E.; Klein, W.M.; Plowman, T.; Lockwood, T.E. Cannabis: an example of taxonomic neglet. *Cannabis Cult.* **1975**, 21–38.
10. Cortes, J.G.; Ryu, B.R.; Pauli, C.; Barroso, L.R.; Park, S.H. Industrial applications of hemp fibre in Europe and evolving regulatory landscape. *J. Nat. Fibers*, **2024**, *21*(1), 2435047.
11. Industrial Hemp Market Size & Share | Industry Report, 2030, accessed 05/12/2025.
12. The World's Top 5 Hemp-Producing Countries - CBD World News, accessed 05/12/2025.
13. Oyarzun, M.; Saalbrink, J.; Bonilla, J.C.; Gouseti, O.; Jensen, P.E.; Risbo, J. Simultaneous extraction of hempseed oil bodies and protein concentrate through mild phytate-driven water-only fractionation. *Future Foods*, 2025, doi: <https://doi.org/10.1016/j.fufo.2025.100864>.

14. Yano, H.; Fu, W. Hemp: A sustainable plant with high industrial value in food processing. *Foods*. **2023**, *12*(3), 651.
15. Small, E. *Cannabis: A Complete Guide*. CRC Press Taylor and Francis Group, Boca Raton, FL (2017).
16. Muangrat, R.; Kaikongjanat, A. Comparative evaluation of hemp seed oil yield and physicochemical properties using supercritical CO₂, accelerated hexane, and screw press extraction techniques. *Journal of Agriculture and Food Research*. **2025**, *19*, 101618.
17. Alonso-Esteban, J.I.; González-Fernández, M.J.; Fabrikov, D.; de Cortes Sánchez-Mata, M.; Torija-Isasa, E.; Guil-Guerrero, J.L. Fatty acids and minor functional compounds of hemp (*Cannabis sativa* L.) seeds and other Cannabaceae species. *J. Food Compos. Anal.* **2023**, *115*, 104962.
18. Farinon, B.; Molinari, R.; Costantini, L.; Merendino, N. The seed of industrial hemp (*Cannabis sativa* L.): Nutritional quality and potential functionality for human health and nutrition. *Nutrients*. **2020**, *12*(7), 1935.
19. Abdollahi, M.; Sefidkon, F.; Calagari, M.; Mousavi, A.; Mahomoodally, M.F. A comparative study of seed yield and oil composition of four cultivars of hemp (*Cannabis sativa* L.) grown from three regions in northern Iran. *Ind. Crops Prod.* **2020**, *152*, 112397.
20. Todorovic, Z.B.; Mitrovic, P.M.; Zlatkovic, V.; Grahovac, N.L.; Bankovic-Ilic, I.B.; Troter, D.Z.; Marjanovic-Jeromela, A.M.; Veljkovic, V.B. Optimization of oil recovery from oilseed rape by cold pressing using statistical modeling. *J. Food Meas. Char.* **2024**, *18*, 474–488.
21. Gaikwad, R.K.; Mondal, I.H.; Dash, K.K.; Shaikh, A.M.; Béla, K. Effectiveness of sustainable oil extraction techniques: A comprehensive review. *Journal of Agriculture and Food Research*. **2025**, *19*, 101546.
22. Devi, M.P.; Ghosh, S.K.; Bhowmick, N.; Chakrabarty, S. Essential oil: its economic aspect, extraction, importance, uses, hazards and quality. *Value Addition of Horticultural Crops: Recent Trends and Future Directions*. **2015**, 269–278.
23. Kant, R.; Kumar, A. Review on essential oil extraction from aromatic and medicinal plants: techniques, performance and economic analysis. *Sustain. Chem. Pharm.* **2022**, *30*, 100829.
24. Rakhee, Mishra, J.; Sharma, R.K.; Misra, K. Characterization techniques for herbal products. *Management of High Altitude Pathophysiology*. **2018**, 171–202.
25. Ali, M.K.; Jon, P.H.; Shourove, J.H.; Rahman, O.; Islam, G.M.R. Optimization of sonication-assisted hydrodistillation for essential oil extraction from *Citrus macroptera* peel: A comparative study of RSM and ANN. *Applied Food Research*. **2025**, *5*, 101446.
26. Jadhav, J.J.; Jadeja, G.C.; Desai, M.A. Ultrasound-assisted hydrodistillation for extraction of essential oil from clove buds—A step towards process improvement and sustainable outcome. *Chemical Engineering and Processing – Process Intensification*. **2023**, *189*, 109404.
27. Ghazanfari, N.; Yazdi, F.T.; Morazavi, S.A.; Mohammadi, M. Using pulsed electric field pre-treatment to optimize coriander seeds essential oil antimicrobial properties, antioxidant activity, and essential oil compositions. *Lebensm. Wiss. Technol.* **2023**, *182*, 114852.
28. Ranjha, M.M.A.N.; Zahra, S.M.; Irfan, S.; Shafique, B.; Noreen, R.; Alahmad, U.F.; Liaqat, S.; Umar, S. Extraction and analysis of essential oils: extraction methods used at laboratory and industrial level and chemical analysis. *Essential Oils: Extraction, Characterization and Applications*. **2023**, 37–52.
29. Aytac, E. Comparison of extraction methods of virgin coconut oil: cold press, soxhlet and supercritical fluid extraction. *Separation Science and Technology*. **2022**, *57*(3), 426–432.
30. Martínez-Abad, A.; Ramos, M.; Hamzaoui, M.; Kohnen, S.; Jiménez, A.; Garrigos, M.C. Optimization of sequential microwave-assisted extraction of essential oil and pigment from lemon peels waste. *Foods*. **2020**, *9*, 1493.
31. Mohamad, N.; Ramli, N.; Abd-Aziz, S.; Ibrahim, M.F. Comparison of hydro-distillation, hydro-distillation with enzyme-assisted and supercritical fluid for the extraction of essential oil from pineapple peels. *3 Biotech*. **2019**, *9*, 1–9.
32. Apetroaei, V.T.; Pricop, E.M.; Istrati, D.I.; Vizireanu, C. Hemp seeds (*Cannabis sativa* L.) as a valuable source of natural ingredients for functional foods – a review. *Molecules*. **2024**, *29*, 2097.
33. Cravotto, C.; Fabiano-Tixier, A.S.; Bartier, M.; Claux, M.; Tabasso, S. Green extraction of hemp seeds cake (*Cannabis sativa* L.) with 2-methyloxolane: a response surface optimization study. *Sustain. Chem. Pharm.* **2024**, *39*, 101509.

34. Baldino, N.; Carnevale, I.; Miletì, O.; Aiello, D.; Lupi, F.R.; Napoli, A.; Gabriele, D. Hemp seed oil extraction and stable emulsion formulation with hemp protein isolates. *Appl. Sci.* **2022**, *12*(23), 11921.

35. Soroush, D.R.; Solaimanimehr, S.; Azizkhani, M.; Kenari, R.E.; Dehghan, B.; Mohammadi, G.; Sadeghi, E. Optimization of microwave-assisted solvent extraction of hemp (*Cannabis sativa* L.) seed oil using RSM: evaluation of oil quality. *J. Food Meas. Char.* **2021**, *15*, 5191–5202.

36. Suarez-Jacobo, A.D.; Pacheco, A.D.; Bonales-Alatorre, E.; Castillo-Herrera, G.A.; Garcia-Fajardo, J.A. Cannabis extraction technologies: impact of research and value addition in Latin America. *Molecules* **2023**, *28*(7), 2895.

37. Munson-Mcgee, S.H. D-optimal experimental designs for uniaxial expression. *J. Food Process Eng.* **2014**, *37*, 248–256.

38. Kabutey, A.; Kibret, S.H.; Kiros, A.W.; Afework, M.A.; Onwuka, M.; Raj, A. Comparative Analysis of Pretreatment Methods for Processing Bulk Flax and Hemp Oilseeds Under Uniaxial Compression. *Foods* **2025**, *14*, 629.

39. Demirel, C.; Kabutey, A.; Herák, D.; Sedláček, A.; Mizera, Č.; Dajbych, O. Using Box–Behnken Design Coupled with Response Surface Methodology for Optimizing Rapeseed Oil Expression Parameters under Heating and Freezing Conditions. *Processes* **2022**, *10*, 490.

40. Kabutey, A.; Mizera, Č.; Dajbych, O.; Hrabě, P.; Herák, D.; Demirel, C. Modelling and Optimization of Processing Factors of Pumpkin Seeds Oil Extraction under Uniaxial Loading. *Processes* **2021**, *9*, 540.

41. Gürdil, G.A.K.; Kabutey, A.; Selvi, K.Ç.; Mizera, Č.; Herák, D.; Fraňková, A. Evaluation of Postharvest Processing of Hazelnut Kernel Oil Extraction Using Uniaxial Pressure and Organic Solvent. *Processes* **2020**, *8*, 957.

42. Divisova, M.; Herak, D.; Kabutey, A.; Sigalingging, R.; Svatonova, T. Deformation curve characteristics of rapeseeds and sunflower seeds under compression loading. *Sci. Agric. Bohem.* **2014**, *45*, 180–186.

43. Herak, D.; Kabutey, A.; Divisova, M.; Simanjuntak, S. Mathematical model of mechanical behaviour of *Jatropha curcas* L. Seeds under compression loading. *Biosystems Engineering*, **2013**, *114*(3), 279–288.

44. Saady, N.M.C.; Nazifa, T.H. Kiwi peel waste enhances manure protein degradation: Statistical optimization using Box–Behnken design and response surface methodology. *Cleaner Waste Systems*. **2025**, *12*, 100385.

45. Thapa, D.; Kumar, V.; Naik, B.; Gupta, A.K.; Richa, R. Process optimization and characterization of *Shorea robusta* (Sal) seed oil using response surface methodology: A sustainable approach to oil valorization. *Food Chemistry: X*. **2024**, <https://doi.org/10.1016/j.fochx.2025.103380>.

46. Weremfo, A.; Abassah-Oppong, S.; Adulley, F.; Dabie, K.; Seidu-Larry, S. Response surface methodology as a tool to optimize the extraction of bioactive compounds from plant sources. *J. Sci. Food. Agric.* **2023**, *103*, 26–36.

47. Avramovic, J.M.; Radosavljevic, D.B.; Velickovic, A.V.; Stojkovic, I.J.; Stamenkovic, O.S.; Veljkovic, V.B. Statistical modeling and optimization of ultrasound-assisted biodiesel production using various experimental designs. *Zastita Materijala*. **2019**, *60*(1), 70–80.

48. Polat, S.; Sayan, P. Application of response surface methodology with a Box–Behnken design for struvite precipitation. *Advanced Powder Technology*. **2019**, *30*, 2396–2407.

49. Veljkovic, V.B.; Velickovic, A.V.; Avramovic, J.M.; Stamenkovic, O.S. Modeling of biodiesel production: Performance comparison of Box–Behnken, face central composite and full factorial design. *Chinese Journal of Chemical Engineering*. **2019**, *27*, 1690–1698.

50. Stamenković, O. S.; Kostić, M. D.; Radosavljević, D. B.; Veljković, V. B. Comparison of box-behnken, face central composite and full factorial designs in optimization of hempseed oil extraction by n-hexane: a case study. *Periodica Polytechnica Chemical Engineering*. **2018**, *62*(3), 359–367.

51. Das, S.; Mishra, S. Box–Behnken statistical design to optimize preparation of activated carbon from *Limonia acidissima* shell with desirability approach. *Journal of Environmental Chemical Engineering*. **2017**, *3*, 588–600.

52. Ye, Z.; Wang, W.; Yuan, Q.; Ye, H.; Sun, Y.; Zhang, H.; Zeng, X. Box–Behnken design for extraction optimization, characterization and in vitro antioxidant activity of *Cicer arietinum* L. hull polysaccharides. *Carbohydrate Polymers*. **2016**, *147*, 354–364.

53. Blahovec, J. *Agromaterials Study Guide*; Czech University of Life Sciences Prague: Prague, Czech Republic, 2008.

54. IS:3579; Indian Standard Methods for Analysis of Oilseeds. Indian Standard Institute: New Delhi, India, 1996.

55. Fornasari et al. Efficiency of the use of solvents in vegetable oil extraction at olaginous crops. *Renewable and Sustainable Energy Reviews*. 2017, 80, 121–124.

56. Niu, L.; Li, J.; Chen, M.-S.; Xu, Z.-F. Determination of oil contents in Sacha inchi (*Plukenetia volubilis*) seeds at different developmental stages by two methods: Soxhlet extraction and time-domain nuclear magnetic resonance. *Ind Crop. Prod.* 2014, 56, 187–190.

57. Danlami, J.M.; Arsal, A.; Zaini, M.A.A. Characterization and process optimization of castor oil (*Ricinus communis L.*) extracted by the Soxhlet method using polar and non-polar solvents. *J. Taiwan Inst. Chem Eng.* 2015, 47, 99–104.

58. Chanioti, S.; Tzia, C. Optimization of ultrasound-assisted extraction of oil from olive pomace using response surface technology: Oil recovery, unsaponifiable matter, total phenol content and antioxidant activity. *LWT Food Sci. Technol.* 2017, 79, 178–189.

59. Ocholi, O.; Menkiti, M.; Auta, M.; Ezemagu, I. Optimization of the operating parameters for the extractive synthesis of biolubricant from sesame seed oil via response surface methodology. *Egypt. J. Pet.* 2018, 27, 265–275.

60. Deli, S.; Farah Masturah, M.; Tajul Aris, Y.; Wan Nadiah, W.A. The effects of physical parameters of the screw press oil expeller on oil yield from *Nigella sativa* L. seeds. *Int. Food Res. J.* 2011, 18, 1367–1373.

61. Hernandez-Santos, B.; Rodriguez-Miranda, J.; Herman-Lara, E.; Torruco-Uco, J.G.; Carmona-Garcia, R.; Juarez-Barrientos, J.M.; Chavez-Zamudio, R.; Martinez-Sanchez, C.E. Effect of oil extraction assisted by ultrasound on the physicochemical properties and fatty acid profile of pumpkin seed oil (*Cucurbita pepo*). *Ultrason Sonochem.* 2016, 31, 429–436.

62. Herak, D.; Kabutey, A.; Sedlacek, A.; Gurdil, G. Mechanical behaviour of several layers of selected plant seeds under compression loading. *Res. Agr. Eng.* 2012, 58(1), 24–29.

63. Lysiak, G. Fracture toughness of pea: Weibull analysis. *Journal of Food Engineering*, 2007, 83(3), 436–443.

64. Gupta, R.K.; Das, S.K. Fracture resistance of sunflower seed and kernel to compressive loading. *Journal of Food Engineering*, 2000, 46(1), 1–8.

65. Herak, D.; Kabutey, A.; Choteborsky, R.; Petru, M.; Sigalingging, R. Mathematical models describing the relaxation behaviour of *Jatropha curcas* L. bulk seeds under axial compression. *Biosyst. Eng.* 2015, 131, 77–83.

66. Chakespari, A.G.; Rajabipour, A.; Mobli, H. Strength behaviour study of apples (cv. Shafi Abadi & Golab Kohanz) under compression loading. *Modern Applied Science*, 2010, 4(7), 173–182.

67. StatSoft Inc. (1995). *STATISTICA for Windows*; StatSoft Inc.: Tulsa, OK, USA, 2013.

68. Pritchard, P.J. *Mathcad: A Tool for Engineering Problem Solving*; McGraw-Hill: New York, NY, USA, 1998.

69. Bambogye, A.I.; Adejumo, O.I. Effects of processing parameters of Roselle seed on its oil yield. *Int. J. Agric. Biol. Eng.* 2011, 4, 82–86.

70. Moslavac, T.; Jokic, S.; Subaric, D.; Ostojcic, M.; Tomas, S.; Kovac, M.; Budzaki, S. Influence of drying, pressing, and antioxidants on yield and oxidative stability of cold pressing oils. *Kem. Ind.* 2023, 72, 433–442.

71. Bogaert, L.; Mathieu, T.; Mhemdi, H.; Vorobiev, E. Characterization of oilseeds mechanical expression in an instrumental pilot screw press. *Ind. Crop Prod.* 2018, 121, 106–113.

72. Baidhe, E.; Clementson, C.L. Modelling rupture and relaxation characteristics of soyabean under compressive loading. *Biosystems Engineering*, 2025, 254, 104137.

73. Sigalingging, R.; Herak, D.; Kabutey, A.; Dajbych, O.; Hrabe, P.; Mizera, C. Application of a tangent curve mathematical model for analysis of the mechanical behaviour of sunflower bulk seeds. *International Agrophysics*, 2015, 29, 517–524.

74. Musayev, M.; Kabutey, A.; Soe, S.S.; Kibret, S.H. Optimization of input factor levels for processing bulk hemp seeds under linear pressing. In: TAE 2025 – 9th International Conference on Trends in Agricultural Engineering, Prague, Czech Republic, 17-19, September 2025.

Disclaimer/Publisher's Note: The statements, opinions and data contained in all publications are solely those of the individual author(s) and contributor(s) and not of MDPI and/or the editor(s). MDPI and/or the editor(s)

disclaim responsibility for any injury to people or property resulting from any ideas, methods, instructions or products referred to in the content.